Hindawi Publishing Corporation
ISRN Civil Engineering
Volume 2013, Article ID 282743, 8 pages
http://dx.doi.org/10.1155/2013/282743

Research Article

Infiltration Kinetics of Wetting in a Building Plaster and the Effect of Added Glass and Hemp Fibers

Serge Gassita,[1] Laurent Marmoret,[1] Anne Perwuelz,[2] and Hassen Beji[1]

[1] *Laboratoire des Technologies Innovantes, Université de Picardie Jules Verne, IUT Génie Civil, Avenue des facultés, le bailly, 80025 Amiens, France*
[2] *Laboratoire GEMTEX, Ecole Nationale des Arts et Industries Textiles (ENSAIT), 2 allée Louise et Victor Champier, BP 30329, 59056 Roubaix Cedex 1, France*

Correspondence should be addressed to Laurent Marmoret; laurent.marmoret@u-picardie.fr

Received 28 November 2012; Accepted 25 January 2013

Academic Editors: S. Easa, C. Mazzotti, and A. A. Torres-Acosta

Capillary rise is an important cause of deterioration for plaster in building. This phenomenon has been studied by the tensiometric experimental technique. Structural and hydric characteristics of plaster have been determined. Decane, a perfectly impregnate fluid, has been used to calculate the porous constant characteristic called C_m and other structural parameters like pore radius and specific surface. Evaluation of the sensibility of plaster for water has been evaluated in a second time. The angle constant and the capillary moisture content have been determined. A comparison between results for plaster and composite plaster with fiber has been done. The addition of glass and hemp fiber does not have important effect on hydric properties (angle constant), but we have observed influence on structural charecteristics (pore radius, porosity, and degree of heterogeneity).

1. Introduction

Most building materials are porous allowing damp from the ground to rise by capillary action. Brick, stone, plaster, and mortar are particularly susceptible to this form of absorption although levels of porosity vary [1]. These building materials, particularly minerals, are deficient in their crystal system that result in surface charges that attract molecules of a dipolar solvent such as water [2]. The plaster is likely to absorb moisture in significant quantity that can shorten its life but also deteriorates the durability of the buildings walls and indoor air quality. Various studies have demonstrated the influence of water (liquid and vapor phases) on the mechanical properties [3, 4] and thermal properties [5].

Washburn's equation is a basic instrument for analysis of height penetration and mass gain of wetting liquids in time inside porous media. Experimental method based on capillary rise is also widely used for porous media characterization (i.e., pore radius and contact angle) [6].

The objective of the work is to use this experimental technique (the so-called tensiometry) to study the behavior of plaster during capillary imbibition. In the first time, structural (pore radius, porosity, and specific surface) and hydric (contact angle and moisture content) properties will be determined. Then, the influence of added glass and hemp fibers will be evaluated.

2. Theory of Capillary Imbibition

The surface tension is defined to express the cohesion of a condensed material [7]. By introducing the surface tension γ_{SV} and $\gamma_{SL}\gamma_{LV}$ as forces per unit length ($N \cdot m^{-1}$), respectively, appearing at the interface solid/vapor, solid/liquid, and liquid/vapor can be defined spread (S) as the parameter comparing the surface energies of the dry solid and wet solid as follows:

$$S = \gamma_{SV} - \gamma_{SL} - \gamma_{LV}. \quad (1)$$

If the sign of the spread S is positive, the material lowered its energy by being wet, and we speak of complete wetting, whereas if otherwise ($S < 0$) wetting is only partial and

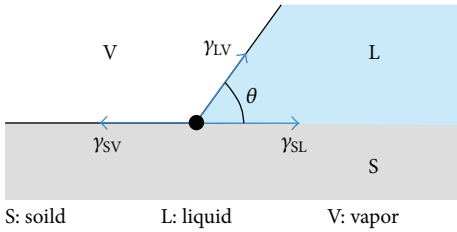

Figure 1: Surface tensions and contact angle [8].

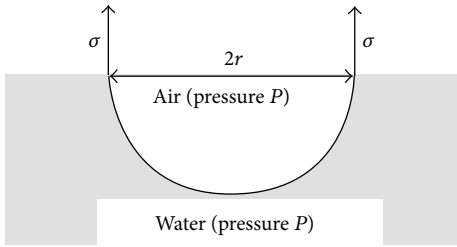

Figure 2: Fluid (water)/air interfaces.

the liquid remains dropped. In the case of partial wetting, the pressure at the liquid-vapor interface is uniform and fixed by the following law of Laplace:

$$P = P_o + \frac{2 \cdot \gamma_{LV}}{r}, \tag{2}$$

where P_o is the atmospheric pressure (Pa) and r is the mean radius of the capillary (m). A combination of the three surface tensions allows knowing the contact angle between the solid and the drop water. Their projection on the contact line (Figure 1) leads to the following relationship of Young:

$$\cos\theta = \frac{\gamma_{SV} - \gamma_{SL}}{\gamma_{LV}} = 1 + \frac{S}{\gamma_{LV}}. \tag{3}$$

The wetting fluid tends to spread over the solid surface [8] with a contact angle θ and then because of the porosity to penetrate into the porous structure by capillarity. When equilibrium is reached, a meniscus is formed at the fluid/air interface between the pressures P (water) and P' (air) in the porous structure (Figure 2). The contact angle (θ) is introduced characterizing the nature of wettability of the solid relative to the liquid/gas contact. If $\theta \leq 90^\circ$, the liquid is considered wetting (especially for $\theta = 0$ where the fluid is perfectly wetting) while for $\theta > 90^\circ$ the liquid is considered nonwetting.

In a steady state, the pressure of the gaseous phase (in general atmosphere, P_{air}) is larger than the other side of the meniscus in the liquid (P_{Liq}). This pressure difference applied to the surface of radius r of the meniscus leads to Laplace's law as

$$\Delta P = P_c = P_{air} - P_{Liq} = \frac{2 \cdot \gamma_{LV} \cdot \cos\theta}{r}, \tag{4}$$

where γ_{LV} is surface tension ($N \cdot m^{-1}$), r is capillary radius (m), and θ is contact angle ($^\circ$). The pressure difference

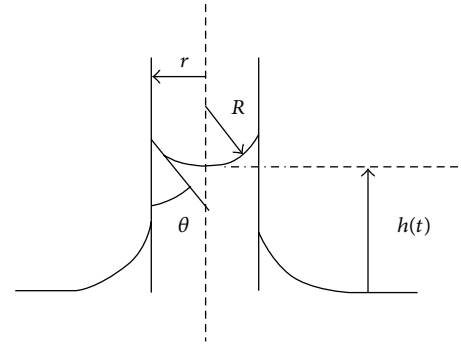

Figure 3: Growth of a capillary liquid in a tube of radius r.

between the gas phase and the liquid phase (ΔP) in a porous medium is wet in the capillary pressure (P_c). Poiseuille's law describes the amount of water absorbed by applying a pressure gradient (ΔP) to the solid liquid interface. The pressure gradient can be defined using the pressure generated by gravity ($\rho \cdot g \cdot h$) and the Laplace pressure as follows:

$$\frac{2 \cdot \gamma_L \cdot \cos\theta}{r}. \tag{5}$$

The hypothesis concerned the existence of the laminar regime, the presence of Newtonian fluid, and the assumed the porous network composed of cylindrical capillary of radius r as

$$\begin{aligned} v = \frac{dh}{dt} &= \frac{r^2}{8 \cdot \eta \cdot h} \cdot \Delta P \\ &= \frac{r^2}{8 \cdot \eta \cdot h} \cdot \left[\frac{2 \cdot \gamma_L \cdot \cos\theta_c}{r} - \rho \cdot g \cdot h\right], \end{aligned} \tag{6}$$

where h is the minimum height of the fluid at time t (s), η is the fluid viscosity ($m \cdot Pa \cdot s$), γ_L is the surface tension (mNm^{-1}), θ is the contact angle ($^\circ$), ρ = density of fluid ($kg\,m^{-3}$), and g is the acceleration due to gravity ($m \cdot s^{-2}$). The porous medium is supposed to be isotropic and rights equivalent to the capillaries of radius r (Figure 3). This mean radius of the capillaries is different from the radius of curvature R of the meniscus. In the first moment of water absorption, h is small, the gravitational force is negligible and, therefore, the integration of (6) leads to the following Washburn equation:

$$h^2 = \frac{r \cdot \gamma_l \cdot \cos\theta}{2 \cdot \eta} \cdot t. \tag{7}$$

Thus, the capillaries are parallel and the same radius, h^2, varies linearly with time.

3. Experimental Techniques

3.1. Material

3.1.1. Plaster. Plaster commercialized under the reference "Targa" by Lafarge that has published some characteristics

Table 1: General characteristics of Targa plaster.

	Density ($kg \cdot m^{-3}$)	Saturated moisture content θ_{sat} ($m^3 \cdot m^{-3}$)
Targa plaster	994 ± 1	0.335 ± 0.010

Table 2: General characteristics of composites plaster fibers.

	Density ($kg \cdot m^{-3}$)	Saturated moisture content θ_{sat} ($m^3 \cdot m^{-3}$)
PGF*	1009 ± 1	0.447 ± 0.010
PHF**	984 ± 1	0.451 ± 0.010

*PGF: plaster added with glass fiber.
**PHF: plaster added with hemp fiber.

[10, 11]. It can be considered as a traditional plaster for coating in building wall. To prepare the samples, the gypsum powder is poured into distilled water taking care not to incorporate too many air bubbles and they are mixed during 30 seconds. The paste stays for 1 minute to be entirely in contact with water before being mixed for 30 seconds. The paste is again allowed to stand for 2 minutes before being placed into the molds. The paste is leveled when it is sufficiently viscous (after about 5 minutes to a mixing ratio water-gypsum plaster: $E/P = 0.8$). The samples were then dried in an oven at a maximum temperature of 45°C until constant mass.

The apparent densities were determined for volume by a caliper with accuracy of 10^{-5} m and for the mass by a balance with an accuracy of 0.1 mg. The total porosity is obtained immersing the material in distilled water after making a previous vacuum. Total porosity is equal to saturated water content (θ_{sat}). Realizing this vacuum avoids the presence of pockets of trapped air in the pores and allows water to more easily access some pores (Table 1).

3.1.2. Fibers. The fibers used are from nonwoven materials used for the insulation of building walls. Two types of fibers are used: a glass fiber and hemp fibers. Structural and hydric characteristics on the glass fiber [12] and on the hemp fiber [13] have been already published. The literature gives the density for the glass fiber (E type) of 2600 $kg \cdot m^{-3}$ and for hemp fibers between 1000 and 1500 $kg \cdot m^{-3}$.

3.1.3. Plaster-Fiber Composite. After this phase, the fibers are embedded in the bulk paste. A new mixing is done during 30 seconds. The samples are placed inside an oven regulated at 45°C maximum until mass constant is obtained. The difficulty in making composites comes from the mixing of fibers in the gypsum slurry and especially the preparation of fibers. And the glass fibers of hemp must be cut before being introduced into the dough. The glass fiber has a length of 1 mm while that of hemp fiber is 1 cm. These dimensions were chosen to obtain a better distribution of the fibers in the paste and to avoid making a fiber block producing a structural heterogeneity in the material. A rasp was used to cut glass wool and to obtain regular fiber length (Figure 4). Cutting hemp fibers

Figure 4: Image of the prepared glass fibers.

Figure 5: Image of the prepared hemp fibers.

is very difficult; an individual separation of the fibers by a chisel was used (Figure 5). We chose a fiber volume fraction 20%. This proportion is the maximum value generally used in the literature [14] to produce a significant effect on the (mechanical) characteristics studied.

No chemical or physical treatment was applied on wool to remove their sizing for instance. This choice corresponds to our desire to use fibers that can come directly from construction waste of glass fiber (PGF).

The addition of hemp fiber (PHF) on plastered matrix decreases the density of the matrix. The addition of glass fibers increases the density of the matrix. We can attribute this difference to the density of the hemp fiber (about 1150 $kg\,m^{-3}$ and the density of glass fiber (2540 $kg\,m^{-3}$). Note that this variation of density does not affect the total porosity. It is stable with and without the addition of fibers. Taking into account the measurement errors by the precision balance, a 2% uncertainty is considered. Thus, the observed deviation of 1% on the measure is not significant (Table 2).

3.2. Tensiometer. A tensiometer, distributed in France by GBX Instruments and referenced to as 3S, was used. The material, originally dry, is weighed and suspended above the fluid (Figure 6) in a closed chamber to reduce the surface exchange by convection. Few minutes are the waiting period

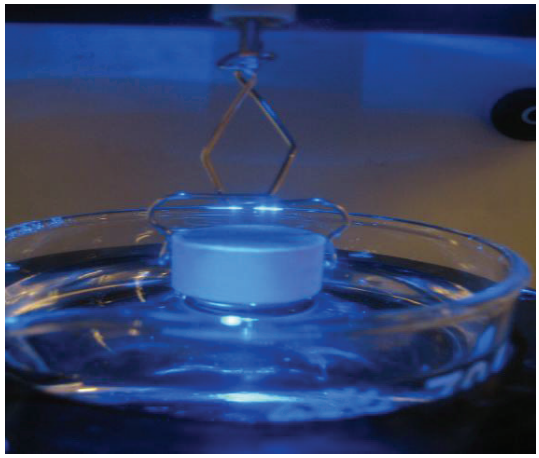

Figure 6: Image of the material suspended above the fluid.

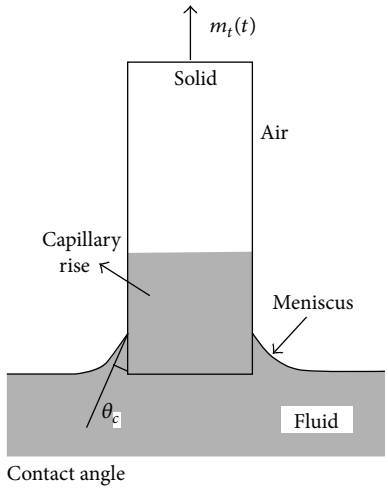

Figure 7: Schematization of the phenomenon of capillary imbibition.

in order to reach an equilibrium thermofluid operation between the material and the ambient climatic conditions. The container containing the fluid is then moved to the maximum speed of 100 μm·s^{-1} until a contact is established between the material and the fluid. A meniscus (Figure 7) appears above the contact surface and, at the same time, the fluid is absorbed in the material due to capillary pressure.

Total mass (m_t, sample mass and absorbed liquid mass) is measured by the balance of the tensiometer (accuracy of 10^{-4} g) and a computer records the measurements every 0.2 s. This mass is composed of two elements: first, the mass of wetting due to the meniscus (m_w) assumed which is constant during the test and also the mass of liquid absorbed in the material (m_a). The total mass m_t is the sum of these two masses m_w and m_a as

$$m_t(t) = m_w + m_a(t). \tag{8}$$

Experimentally, the total mass m_t is measured by the balance of the tensiometer. After subtracting the mass of the meniscus, the absorbed mass (m_a) by the sample as a function of time is determined. The water height (h) can be deduced from the mass by the following relation:

$$m_a = \rho \cdot h \cdot \varepsilon \cdot A, \tag{9}$$

where ε is the total porosity (%) and A is the exchange surface of the porous medium (m^2) with water.

For the same sample as previously described, the maximum height growth is reached when the liquid is at equilibrium ($dh/dt = 0$ in (6)). The equilibrium height h_{eq} is described by Jurin's law as

$$h_{\text{eq}} = \frac{2 \cdot \gamma_L \cdot \cos\theta_c}{\rho_l \cdot g \cdot r}. \tag{10}$$

Table 3: Decane properties.

σ (mN·m^{-1})	η (mPa · s)	ρ (kg · m^{-3})
23.6	0.910	730

4. Experimental Results

4.1. Results with Decane as a Perfectly Wetting Fluid ($\theta_c = 0^\circ$). Decane is a perfectly wetting fluid so the contact angle (θ_c) between the fluid and the material is zero. The surface energy (σ) of decane (also called surface tension), given by the manufacturer, has been checked experimentally by using a platinum plate tensiometer. The viscosity (η) and density (ρ) are provided by the manufacturer (Table 3).

Combining (7) and (9), the kinetics of weight gain as a function of time can be described by

$$m_a^2 = \frac{C_m \cdot \rho^2 \cdot \gamma_L \cdot \cos\theta_c}{\eta} \cdot t = a_1 \cdot t. \tag{11}$$

This equation is very important in the tensiometry processing because it allows determining the constant parameter C_m which is a characteristic of the porous medium. The slope of the curve representing the square of the absorbed mass (m_a^2) versus time (t) corresponds to the following a_1 parameter:

$$a_1 = \frac{C_m \cdot \rho_l^2 \cdot \gamma_L \cdot \cos\theta_c}{\eta} \tag{12}$$

And from a_1 coefficient, it is possible to determine the characteristic C_m using (12). To calculate the pore radius (r), we use the following equation [6]:

$$C_m = \frac{\varepsilon^2 A^2 r}{2}, \tag{13}$$

where A is the exchange surface of the porous medium (m^2). The specific surface area can be then determined as:

$$S_{\text{SP}} = \frac{1}{\rho_0 \cdot 2 \cdot r}, \tag{14}$$

Table 4: Structural characteristics of the plaster and composites plaster fiber.

Material	C_m (mm^{-5})	r: mean radius of the pores (μm)	Specific area ($m^2 \cdot g^{-1}$)	Fineness ($\times 10^5$ $m^2 \cdot m^{-3}$)
Plaster	0.04 ± 0.02	0.08 ± 0.03	6.3 ± 3.4	1.087 ± 0.212
PGF	0.14 ± 0.09	0.02 ± 0.01	3.3 ± 2.2	0.568 ± 0.112
PHF	0.95 ± 0.30	0.12 ± 0.07	4.3 ± 1.8	0.724 ± 0.142

Table 5: Samples and meniscus characteristics.

Material	Size of the samples				Characteristics of the meniscus				
	Height (mm)	Width (mm)	Thickness (mm)	Perimeter $p = 2\cdots w + 2\cdots e$	k^{-1} (mm)	h_{omax} (mm)	V_A (mm^3)	m_w (mg)	θ_M (°)
Plaster	15.2	50	6	112	2.84	4.01	481	131	0

where ρ_0 is dry density of the material and r is the pore radius. The fineness (F) can be determined by

$$F = \frac{S_{SP} \cdot \rho_0}{1 - \varepsilon}, \tag{15}$$

where ε is the porosity of the material.

Decane has been used as an impregnate liquid and the results are presented in Table 4 for the plaster and composites obtained by the added glass fiber (PGF) and hemp fibers (PHF). Because of the pore radius being greater than 50 (nm), plaster can be considered as composed predominantly of macropores [15]. For similar plasters, pore radius obtained is lower than those reported in the literature [10] using mercury porosimetry (3 and 5 μm). The principle of different measures can explain these variations. Thus, mercury porosimetry has the disadvantage of applying a pressure that may be too large for the pore network and causes cracks but the advantage of mercury is that it is inerted into the material. By tensiometry, the water can dissolve the solids and thus change the pore structure (size and distribution). The addition of hemp fibers (PHF) in the matrix plasterer increases the average size of pore radii, while the addition of glass fibers (PGF) decreases it. We also note that adding fiber (whatever the type of fiber hemp and glass) decreases the surface area resulting in a less finely divided material. The explanation may come from the formulation of our materials. Fiber additions were defined from a base of volume proportion. The average density of hemp fiber (1150 $kg \cdot m^{-3}$) is a half more than the glass fiber one (2540 $kg \cdot m^{-3}$). We have observed by gamadensimetry that addition fiber reduces dissolution of the plaster matrix [16].

Bories [17] has suggested comparing building materials by the use of a figure representing variations depending on fineness against the pore radius. Our materials presenting a very small mean pores radius (pore radius lower than 10^{-7} meter) and high fineness (inducing a finely divided porous network) are denoted as hygroscopic materials.

4.2. Study of the Water Capillary Imbibition. Water is now the impregnant fluid. The study starts by determining the contact angle inside the meniscus (θ_M) and during the capillary imbibition (θ_c). Moisture contents obtained during capillary imbibition and by water saturation are compared.

4.2.1. Meniscus Formation. In general, the duration of a test is between 100 and 600 seconds depending on the materials. The mass of the meniscus (m_w) is assumed to be constant after 1 second. This mass is determined at the end of the test by subtracting the final mass m_t to the mass without any meniscus (fluid absorbed) when the fluid and the material have no contact. Then, the mass of fluid absorbed by the material (m_a) can be studied as a function of time. From the mass of the meniscus and knowing that g is the acceleration due to the gravity, it is possible to determine the contact angle of the meniscus (θ_c) of the plaster as

$$m_w \cdot g = \gamma_L \cdot p \cdot \cos\theta_c. \tag{16}$$

When saturation of the sample in contact with the meniscus is reached (Figure 9), we can define the corresponding volume by the relationship as

$$V_A = \varepsilon \cdot h_o \cdot w \cdot e, \tag{17}$$

where w and e are, respectively, the width and the thickness of the sample measured using a caliper to an accuracy of 10^{-4} m and ε is the total porosity of the material. The meniscus, characterized by its height h, is defined by [18]

$$h_o = \left(\sqrt{2} \cdot \sqrt{1 - \sin\theta}\right) \cdot k^{-1}. \tag{18}$$

The capillary length (k^{-1}) describes the threshold at which gravity becomes important. It is obtained by considering the Laplace pressure and the hydrostatic equilibrium and thus

$$k^{-1} = \sqrt{\frac{\gamma_L}{\rho \cdot g}}. \tag{19}$$

For a sample of rectangular 50 × 6 mm base and 15.2 mm in height, the mass of water absorbed by the meniscus is 131 mg by tensiometry test. It is found (Table 5) that the

Table 6: Contact angle.

Material	Plaster	PGF: plaster added with glass fiber	PHF: plaster added with hemp fiber
θ_c (°)	78.8 ± 18.8	79.0 ± 28.9	77.1 ± 23.0

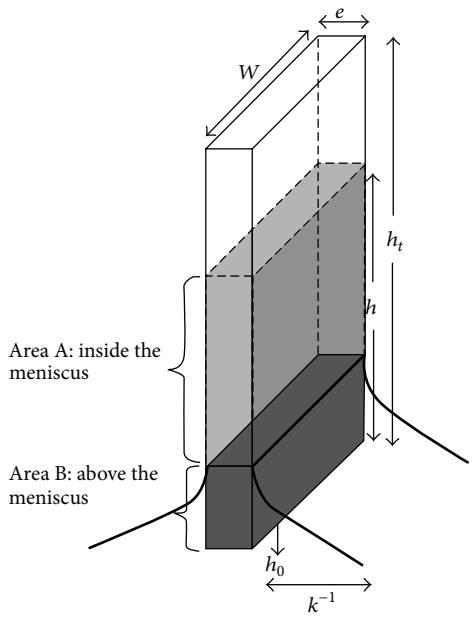

Figure 8: Capillary imbibition in the material [18].

contact angle in the meniscus is zero ($\theta_M = 0°$) which allows to conclude that water is a completely wetting fluid for plaster.

Pore sizes of radius $r < k^{-1}$ and gravity are negligible, and the liquid is weightless and capillary effects are dominant [8]. As capillary length is greater than pore radius (Table 5), gravity has been considered as negligible (Figure 8).

4.2.2. Contact Angle during Capillary Imbibition. As the constant parameter C_m has been already calculated using the decane (Table 4), it is possible to determine the contact angle during the capillary imbibition. During the capillary imbibition, the contact angle is not equal to zero contrary to the result in the meniscus. We can observe (Table 6) that contact angle is quite constant (equal to 80°) with (PGF and PHF) or without fiber added in plastered matrix. Note that the uncertainly (20°) is high coming from the precision of the experiments and the adding of the uncertainly of other parameters needs to be calculated in the angle.

However, our result can be considered coherent with Finot et al. [19] who found an angle of 60° even if it has been obtained by atomic force microscopy (AFM) at the microscopic level.

4.2.3. Capillary Moisture Content. Two distinct areas can be identified in Figure 9. At short times, the mass absorbed

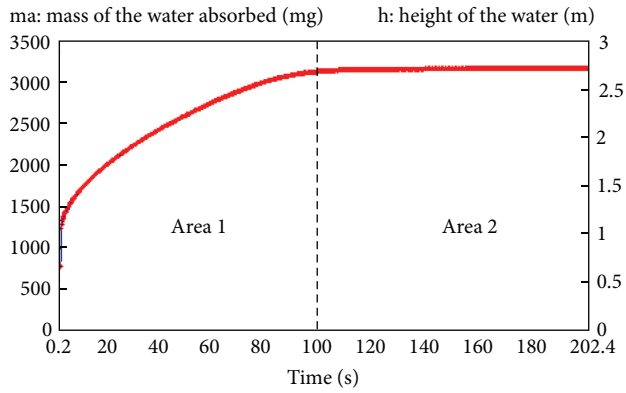

Figure 9: Mass of water absorbed in the plaster.

increases greatly. This phase corresponds to the impregnation fluid in the capillary material (Area 1). Once the capillary fringe reaches the height of the sample, the weight gain becomes very slow (Area 2). This weight gain can be attributed to the diffusion of air bubbles remained trapped in the pore network during water transfer. It is controlled by Fick's law and corresponds to the absorption of trapped porosity [20, 21]. If we let the system evolve, the weight gain tends gradually to saturation of the sample. It is interesting to compare the water content obtained at the end of the test tensiometry and the water content obtained by immersing the sample in water. We can notice that the mass of water absorbed in the sample amounted to about 3207 mg after 100 s (Figure 9) and the equilibrium height obtained is equal to 2.70 cm. This equilibrium height can be reached experimentally because the sample has a total height of 1.52 cm. This explains the sudden break observed in Figure 9 for a time of 100 s. At that time, water saturates the sample reaching the height of the sample which is confirmed visually during the test.

Note that the water content obtained at the end of a test tensiometry, when saturation is reached, is in fact the capillary water content (θ_{cap}). This corresponds to the saturation of the accessible porosity (ε_{cap}) with water at atmospheric pressure and in air that is in two-phase regime (AFNOR B10.513). The immersion of the sample in water which is a wetting fluid for plaster provides the water content to saturation (θ_{sat}). This one gives a good estimate of the total porosity (ε) [9]. However, it is important, before immersion, to empty into the material to be placed in accordance with standard single-phase regime of RILEM (test no. I.1 established in 1978). Hirschwald coefficient is defined as the saturation parameter after 48 hours taking into account the ratio between the accessible porosity to water ε_{acc} and the total porosity ε as

$$S_{48} = \frac{\varepsilon_{acc}}{\varepsilon}. \quad (20)$$

This ratio (Hirschwald coefficient: S_{48}) is used to define the degree of heterogeneity of the porous network of the material. The medium is more homogeneous and more capillary and water content tends toward 1 for the full saturation.

Table 7: Capillary moisture content (θ_{cap}) and saturated moisture content (θ_{sat}).

	θ_{cap}	$\theta_{sat} \approx \varepsilon$	$S_{48} = \theta_{cap}/\theta_{sat}$
Plaster	0.311 ± 0.010	0.335 ± 0.010	92.8%
PGF	0.309 ± 0.010	0.332 ± 0.010	93.0%
PHF	0.296 ± 0.010	0.325 ± 0.010	91.1%

Table 8: Capillary absorption capacity and sorptivity.

	Plaster	PGF	PHF
A_C (kg·m^{-2}·s$^{-0.5}$)	0.416	0.363	0.156
S (cm·s$^{-1/2}$) by (21)	0.099	0.087	0.041
S (cm·s$^{-1/2}$) by gravimetry [9]	0.095	0.096	0.078

The environment is more heterogeneous and this report tends to 0. We observed (Table 7) that the capillary water content is equal to 92.8% of the water content at saturation. We find that adding 20% of volume of fiber has no effect on moisture contents (capillary and at saturation) and on the degree of heterogeneity of the porous network.

4.2.4. Capillary Absorption Capacity. According to RILEM, the test for measuring the capillary absorption coefficient consists of studying the imbibition inside an initially dry sample. The mass gain Δm is recorded versus the square root of time t. A linear variation is obtained and its slope corresponds to the capillary absorption coefficient, A_C (kg·m^{-2} · s$^{-0.5}$). From this coefficient it is possible to determine the sorptivity (S) by

$$A_C = \rho_l \cdot \varepsilon \cdot S. \quad (21)$$

We have validated results by comparing sorptivity (S) with tensiometric technique and by a more traditional method described in [22]. A good coherence can be observed even if difference can be noted for composite plaster-hemp fiber (PHF). Due to the size of the measuring cell, the samples are much smaller for the tensiometric technique. So explication can come from the scale factor or the difficulty to distribute the fibers everywhere inside a small volume. We observed that (Table 8) capillary absorption capacity is more important for plaster than for composite and the addition of hemp fiber decreases this capacity by a factor of 2 than for glass fiber by tensiometric technique. This observation is less important on the sorptivity compared with the traditional method.

5. Conclusion

Capillary rise has been studied by the tensiometric experimental technique. Firstly, by the use of decane, a perfectly impregnant fluid, the porous constant characteristic called C_m, has been determined. A mean pore radius (0.1 μm) has been calculated by the Washburn equation. The addition of glass fiber has decreased the mean pore radius and the fineness. The addition of hemp fiber has increased the mean pore radius and the fineness. We have explained this observation by the difference in the average density of hemp fiber (1150 kg·m^{-3}) which is a half more than the glass fiber one (2540 kg·m^{-3}) and we have taken constant the volume proportion of fiber added. Another explication can be advanced, and by gammadensimetry we have noted that the addition of fiber reduces the dissolution of the matrix. We have obtained a contact angle equal to zero in the meniscus and equal to 80° during capillary imbibition. The addition of 20% of volume of fiber has no effect on the contact angle and on the degree of heterogeneity of the porous network (93%). As the value is near to 1, porous network of the materials can be considered homogeneous. Results with tensiometric technique and a more traditional technique for determining the sorptivity have been compared. A good coherence has been obtained and we observed that the addition of fiber reduces the absorption capacity.

References

[1] L. Pel, *Moisture transport in porous building materials [Ph.D. thesis]*, Eindhoven University, 1995.

[2] E. Goossens and E., *Moisture Transfer Properties of Coated Gypsum*, University press, 2003.

[3] P. Coquard, R. Boistelle, L. Amathieu, and P. Barriac, "Hardness, elasticity modulus and flexion strength of dry set plaster," *Journal of Materials Science*, vol. 29, no. 17, pp. 4611–4617, 1994.

[4] E. Badens, P. Llewellyn, J. M. Fulconis et al., "Study of gypsum dehydration by controlled transformation rate thermal analysis (CRTA)," *Journal of Solid State Chemistry*, vol. 139, no. 1, pp. 37–44, 1998.

[5] D. Quenard, R. Cope, F. Derrien, and H. Sallee, "Influence de la teneur en eau sur la diffusivité thermique du plâtre," *Matériaux et Constructions*, vol. 17, no. 4, pp. 306–309, 1984.

[6] T. Dang-Vu and J. Hupka, "Characterization of porous media by capillary rise method," *Physicochemical Problems of Mineral Processing*, vol. 39, pp. 47–65, 2005.

[7] D. Bonn, J. Eggers, J. Indekeu, and J. Meunier, "Wetting and spreading," *Reviews of Modern Physics*, vol. 81, no. 2, pp. 739–805, 2009.

[8] F. Brochard-Wyart, J. M. di Meglio, and D. Quéré, "Theory of the dynamics of spreading of liquids on fibers," *Journal de Physique Paris*, vol. 51, no. 4, pp. 293–306, 1990.

[9] F. A. L. Dullien, "Capillary effects and multiphase flow in porous media," *Journal of Porous Media*, vol. 1, no. 1, pp. 1–29, 1998.

[10] S. Meille, P. Reynaud, M. Saadaoui, and G. Fantozzi, "Dissipated energy in dry and wet plasters," *Defect and Diffusion Forum*, vol. 206-207, pp. 171–174, 2002.

[11] K. M. Song, J. Mitchell, H. Jaffel, and L. F. Gladden, "Magnetic resonance imaging studies of spontaneous capillary water imbibition in aerated gypsum," *Journal of Physics D*, vol. 44, no. 11, Article ID 115403, 2011.

[12] F. Achchaq, K. Djellab, H. Beji, and L. Marmoret, "Hydric, morphological and thermo-physical characterization of glass wools from macroscopic to microscopic approach," *Construction and Building Materials*, vol. 23, no. 10, pp. 3214–3219, 2009.

[13] F. Achchaq, K. Djellab, L. Marmoret, and H. Beji, "Hydric behavior of a natural composite material: a hemp wool experimental study," *International Review of Civil Engineering*, vol. 1, no. 2, 2010.

[14] P. Boustingorry, P. Grosseau, R. Guyonnet, and B. Guilhot, "The influence of wood aqueous extractives on the hydration kinetics of plaster," *Cement and Concrete Research*, vol. 35, no. 11, pp. 2081–2086, 2005.

[15] D. H. Everett, "Pore systems and their characteristics, Studies in surface science and catalysis," in *Proceedings of the IUPAC Symposium (COPS '87)*, 1987.

[16] S. Gassita, *Contribution à l'étude du transfert hydrique par imbibition d'eau dans une matrice plâtrière avec ajout de fibres [Ph.D. thesis]*, University of Picardie Jules Verne, 2010.

[17] S. Bories, "Recent advances in modelisation of coupled heat and mass transfer in capillary-porous bodies," in *Proceedings of the 6th International Drying Symposium*, pp. 47–61, Versailles, France, 1988.

[18] L. Zhu, A. Perwuelz, M. Lewandowski, and C. Campagne, "Static and dynamic aspects of liquid capillary flow in thermally bonded polyester nonwoven fabrics," *Journal of Adhesion Science and Technology*, vol. 22, no. 7, pp. 745–760, 2008.

[19] E. Finot, E. Lesniewska, J. P. Goudonnet, J. C. Mutin, M. Domenech, and A. At Kadi, "Correlating surface forces with surface reactivity of gypsum crystals by atomic force microscopy. Comparison with rheological properties of plaster," *Solid State Ionics*, vol. 141-142, pp. 39–46, 2001.

[20] P. Bousquié, *Texture et porosité de roches calcaires [Ph.D. thesis]*, Ecole des Mines de Paris, 1979.

[21] J. D. Mertz, *Structures de porosite et proprietes de transport dans les grès*, Universite Louis Pasteur de Strasbourg, Sciences Geologiques, 1991.

[22] S. Gassita, L. Marmoret, H. Ben Hamed, and H. Beji, "Sorptivity and hydraulic diffusivity of coating gypsum and impact of hemp fibers addition," *Defect and Diffusion Forum*, vol. 312–315, pp. 818–823, 2011.